arXiv:1208.2994v2 [cond-mat.mes-hall] 17 Sep 2012

An electron source with high spatial coherence

Josh Y. Mutus, Radovan Urban, Jason Pitters, Lucian Livadaru, Peter A. Legg, and Robert A. Wolkow*
Department of Physics, University of Alberta, 11322-89 Avenue, Edmonton, Alberta, T6G 2G7, Canada and
National Institute for Nanotechnology, National Research Council of Canada,
11421 Saskatchewan Drive, Edmonton, Alberta, T6G 2M9, Canada

This work demonstrates the fabrication of a single atom tip electron source with exceptionally high spatial coherence. A coherence angle of 14.3 ±0.5°was measured, indicating a virtual source size of 1.7 ±0.6 Å. The nanotips under study were crafted using a spatially-confined, field-assisted nitrogen etch, which removes material from the periphery of the tip apex, resulting in a sharp, tungsten-nitride stabilized, high-aspect ratio source. The coherence properties are measured in a low-energy electron point source microscope with a carbon nanotube bundle acting as a bi-prism. This work represents a marked improvement in spatial coherence of electron sources.

Electron sources have had a substantial impact on modern physics, since the invention of the cathode-ray tube well over a century ago. Now, electron sources are ubiquitous in science and industry in variety of areas such as spectroscopy, microscopy and lithography. This diversity of applications calls for a diversity of sources, with different energy distributions, beam currents and coherence properties. There have been sequential innovations in the area of nanotip fabrication and characterisation [1–4]. Nanotips are of interest as electron and as gas field ion sources due to their great brightness and coherence [5–7]. Such sources have many fundamental applications in electron interferometry from the Hanbury-Brown and Twiss experiment to the Ahronov-Bohm [8] effect along with the possibility of probing ultrafast dynamics [9]. However, the spatial coherence of such sources has been limited by low beam divergence angles. Lack of spatial coherence has been found to be the limiting factor in the resolution of single-atom sources in electron holography [10, 11]. To date, ultra-sharp tips made by building up a sharp apex on a relatively broad base have been thoroughly studied.

The development of techniques for creating nanotips that emit electrons from a single terminal atom have been ongoing since the first work by Fink in 1986 [1, 2]. Recently, the latter have been shown to be completely coherent: the emission across the entire opening-angle shares one phase [3]. However, although completely coherent, the emission angle for such tips remains rather small, typically a few degrees [3]. The tip studied here is shown to also be completely coherent, but in addition exhibits an opening angle more than 4 times larger than measured previously.

The degree of spatial coherence of an electron source can be found using a low-energy electron point source (LEEPS) microscope [12]. The LEEPS microscope is shown schematically in Figure 1 and consists of only a source, a sample and a detector. The coherent electron wave scatters off the sample and interferes with the reference wave at the detector to create an interference pattern. The width of the interference pattern is a measure of the width of the coherent wavefront emitted by the tip.

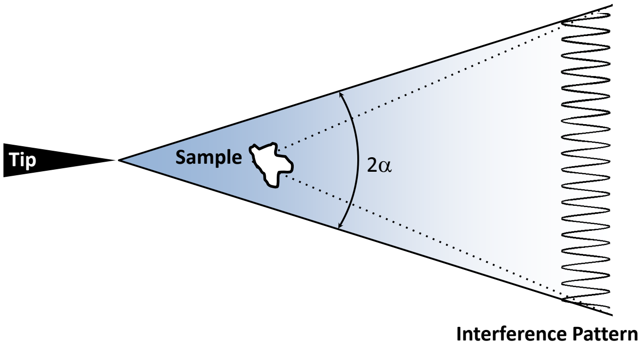

Figure 1: A schematic of the LEEPS microscopy experiment. A sharp tip is brought near a conductive sample, which also serves as anode. A bias is placed between tip and sample, causing electrons to be emitted from the tip, through the sample towards the screen. The result is an interference pattern on the screen. This pattern can be analyzed to deduce quantities about the coherence properties of the beam, the fields the surrounding sample and it's structure. The coherence angle of the beam α can be found by measuring the width of the pattern on the screen. Only coherent portions of the beam will contribute to the overall interference pattern.

As in any microscope, the numerical aperture dictates the resolution. In a LEEPS microscope, the coherence angle, α, is dictated by the character of the source. However, it is limited by many attributes of the microscope itself: uncontrolled fields and mechanical and electrical stability of the instrument can also prevent attainment of a larger coherence angle. The diffraction limited resolution, R, of the LEEPS microscope is given by:

$$R \geq \lambda/2\sin\alpha, \tag{1}$$

where λ is the wavelength of the incident electrons. Another widely used estimate of resolution is the virtual source size, given by [12]:

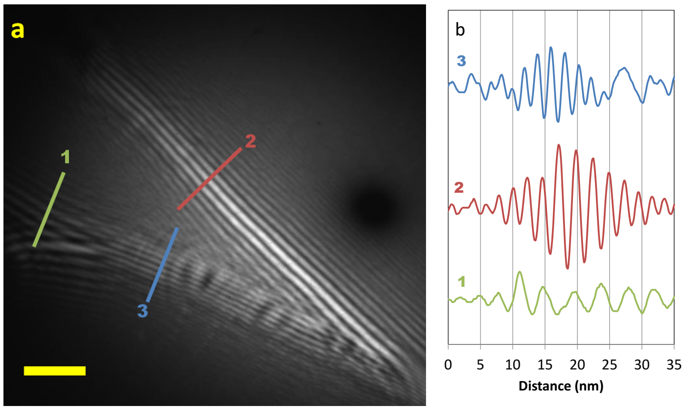

Figure 2: The electron beam forms a broad pattern seen at low magnification, due to simple scattering off the bundle. This is shown in (a) (scale bar 20nm) and the corresponding line profiles in (b) where a branched bundle is imaged. As the branches come together to form wider bundles, the pitch of the pattern becomes finer (from the blue to purple traces in (b)).

$$R_v \approx \lambda/\pi\alpha. \tag{2}$$

In this paper we report on the coherence properties of a nanotip made by removing material from the shank of the tip, rather than building upon it. This technique uses a field-assisted, spatially-confined nitrogen etch and was reported in 2006 [13]. Such tips are not only terminated by a single tungsten atom but are uniquely stable due to the nitrogen-rich layer formed during fabrication, which coats the surface area surrounding the apex. This greatly inhibits metal diffusion and allows the tip to survive exposure to atmosphere and heating to a thousand degrees Celsius.

The coherence properties of the beam were measured using a custom-designed LEEPS microscope [14]. The details of its construction are the subject of a future publication. Here we give a brief description: the tip, sample and motors are contained in the scanning head. The motors are used to position the tip relative to the sample with subnanometre precision. The scanning head is suspended above a (micro-channel plate) MCP. A modest, negative bias voltage (from 60-500V, depending on the separation between tip and sample) is applied to the tip, with the sample grounded. Electrons are field-emitted from the tip, through the sample, towards the MCP some distance away. A magnified image of the region of the sample irradiated by the electrons is projected on the MCP. The image is magnified by the ratio of the tip-sample to the tip-MCP distance. In this work, the tip-MCP distance is (4.0 ± 0.5) cm, but it can be varied easily from 0.5 to 20 cm by moving both tip and sample relative to the MCP.

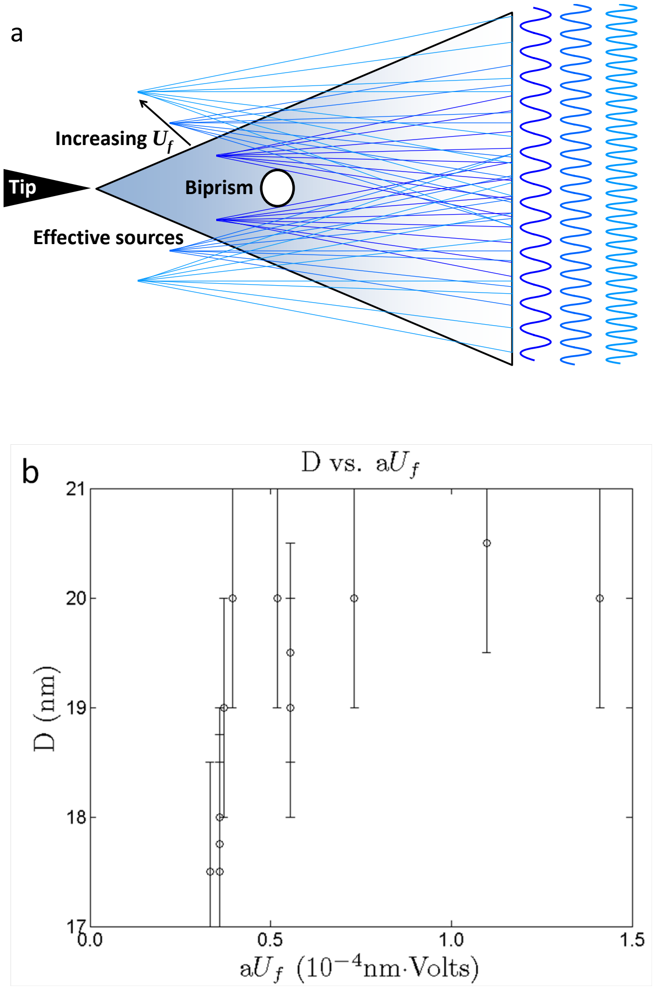

Figure 3: A second interference pattern is generated by electrons that do not directly scatter off the bundle, but instead are deflected by the electric field surrounding it. This results in a bi-prism mode, analogous to that of the double slit, where the effective slit separation can be tuned by changing the bias between the tip and the bundle. This is illustrated in (a) as the field increases, so does the separation of the effective sources, resulting in a finer fringe pattern. (b) demonstrates the dependence of the effective source separation on tip-bundle bias U_f and separation a.

Carbon nanotube bundles were suspended across holes in a 50 nm thick silicon nitride window. These windows were perforated by a regular array of 2 μm holes on a 4 μm pitch [15]. In order to make the windows conductive, they were coated in 5 nm Cr and 45 nm Au. These suspended nanotube bundles were brought into the LEEPS microscope for imaging.

The intereference pattern generated by the LEEPS mi-

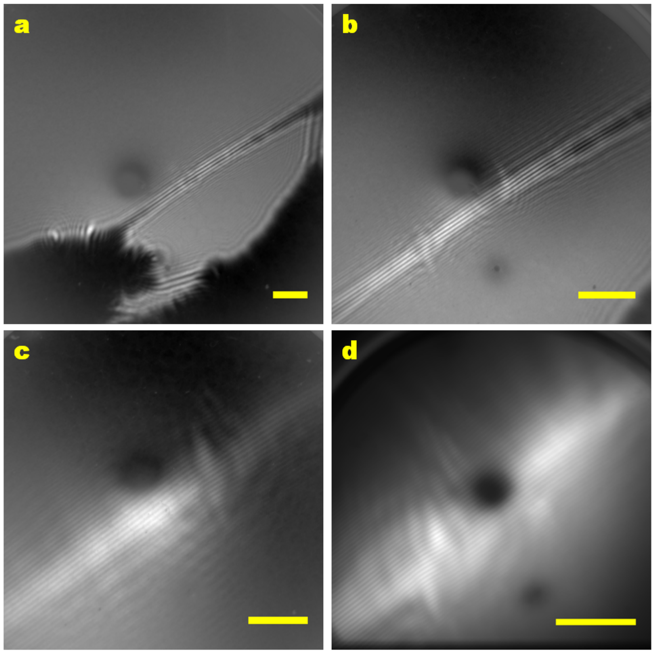

Figure 4: LEEPS images of carbon nanotube bundles: as the tip approaches the bundle, the magnification increases. As the magnification increases, the pattern fills the emission spot on the screen and the beam is said to be completely coherent. Scale bars are 100 nm and 50 nm for a-b and c-d, respectively.

crscope showed two distinct fringe patterns. At low magnifications, diffraction patterns due to direct scattering off the bundle are observed. Such patterns are shown in Figure 2a and the corresponding profiles in 2b.

At higher magnifications, a finer fringe pattern becomes visible. This pattern is thought to be due to electrons being redirected by the nanotube bundle. In transmission electron microscopy, an electron bi-prism is made from a thin, conductive filament, biased between two grounded plates [16]. A carbon nanotube bundle approximates this by having a potential gradient surrounding the bundle. Electrons that do not directly scatter off the bundle are steered by the electric field due to the potential difference between the tip and bundle. As a result, carbon nanotubes are used to tailor the interference of the electron beam in LEEPS [17, 18] and in this work can be used to measure the coherence properties of the beam.

The electron trajectories are bent towards the optical axis by the electric field resulting in an interference pattern analogous to that of the double slit, where the slit separation is tuned by varying the voltage between tip and bundle [19][20]. This is shown schematically in Figure 3a. The angular intensity of the interference pattern can be expressed as:

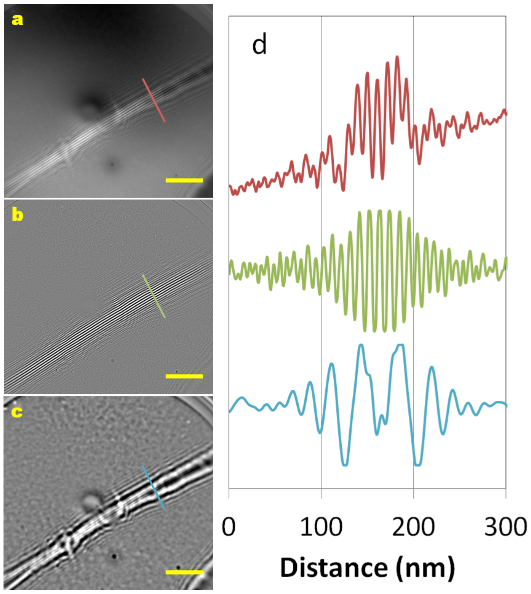

Figure 5: Filtered versions of Figure 4(b) show each fringe pattern is composed of two different set of fringes. Figures (b) and (c) are low-pass and high-pass filtered images of (a). Their respective line profiles are shown in (d) A low frequency set of fringes due to scattering of the bundle itself and a higher frequency set of fringes due to the bi-prism effect. The pitch of the finer set of fringes can be tuned by varying the tip-sample distance and voltage as shown in Figure 3b. Scale bar is 100nm.

$$I(\alpha) = 4I_o \cos^2\left(\frac{4\pi a\gamma_o U_f}{\lambda}\alpha\right), \tag{3}$$

where a is the tip-bundle distance, U_f is the relative bias between tip and sample, λ is the deBroglie wavelength of the electron and γ_o is the angular deflection per Volt characteristic of the bi-prism. The bi-prism can be expressed as a double slit with an effective slit separation of $D = a\gamma_o U_f$. The pitch of the fringe pattern can be changed by tuning the voltage of the tip relative to the bundle, as is shown in Figure 3b. Practically, the tip-sample distance, extraction voltage and current are related by the Fowler-Nordheim equation [21]. The tip can only be operated safely in a narrow window for beam current ranging between 0.03 - 2 nA. This limits the amount we can explore the dependence of the pattern on these variables. These finer fringe patterns are only revealed at higher magnifications and are evident in Figures 4, 5, 6.

A typical series of images is shown in Figure 4. As the tip is moved closer to the bundle, the magnification of the fringe pattern increases. Also, the visibility of the fringes decreases as the magnification increases. This is thought to be due to an increased fraction of the electron

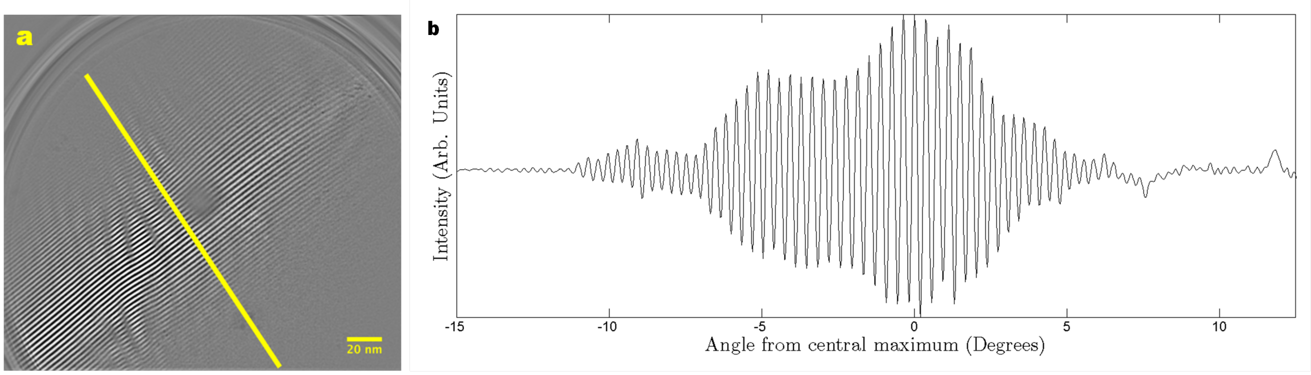

Figure 6: (a) shows a high-pass filtered version of image 4(d) (scale bar is 50nm). The interference pattern fills the detector with high-frequency fringes. High order fringes, not obvious in (a) are visible in the line profile shown in (b). The beam is completely coherent and possesses a coherence angle greater than 14°.

beam being scattered and absorbed by the bundle as the tip approaches.

The different fringe patterns can be seen distinctly by filtering the data as shown in Figure 5 (a-c). The broader set of fringes is thought to be the diffraction pattern from scattering off the bundle. The finer, sinusoidally-spaced fringes are thought to be due to the bi-prism effect described in equation 3. The two sets of fringes can be accentuated by filtering the images. The finer fringes are accentuated by using a high-pass filter, as in Figure 5b.

The coherence angle (α shown in Figure 1) was measured simply by calculating

$$\tan^{-1}(\frac{w}{2L}),$$

where w was the width of the pattern on the MCP and L was the tip-MCP distance. The maxiumum coherence angle for these interference patterns (as shown in Figure 6) was 14.3 ±0.5°. This represents a marked improvement over the previous state of the art.

Using Eq. 2 and these measurements yield a virtual source size [22] of 1.7 ±0.6 Å[12]. Additionally, the upper-bound on resolution of the LEEPS microscope can be estimated using the diffraction limit in Eq. 1. From this we expect a resolution of 2.6 ±0.6 Å.

The reasons for the improvement in coherence angle over previous work is not entirely known. It may be a simple result of the mechanical and electrical stability of the LEEPS microscope. Great care was taken to minimize vibrations of the tip relative to the sample. The instrument has been operated in atom resolving scanning tunneling microscopy mode, demonstrating that vibrations are ∽0.1 Åin magnitude. This may allow the microscope to resolve higher coherence angles than previously reported. Other factors may also contribute to the attainment of higher coherence angles, such as the nature of the tip etching process. The nanotip in this work is made by removing material from the shank of the tip, rather than building a sharp protrusion upon a broad base. This results in a tip with a higher aspect-ratio. The electron emission is expected to be broader for a higher aspect-ratio tip, since an emitter with a larger radius of curvature will focus the emission into a narrow beam [6, 7]. Lastly, the nature of the surface of the tip itself may play a role. As the tip is etched, a protective nitrogen-rich coating remains which modifies the work function of the tip. This through a proximity effect, may play a subtle role in tuning emission character of the tip. Further theoretical studies of these contributing factors are necessary to fully understand the novel properties of the nitrogen etched nano-tip.

Whereas no previously studied point source has displayed greater than 3 degrees coherence opening angle, corresponding to at best 1.5 nm [11] resolution for a LEEPS microscope, the tip described here exhibits greater than 14 degrees opening angle, indicating the potential for ~1.6 Åresolution and a transformative result for electron holography by the LEEPS method. Such measurements are presently underway.

This research was funded by the Natural Sciences and Engineering Research Council and Alberta Innovates - Technology Futures. The authors would like to thank Mark Salomons and Martin Cloutier for their invaluable help in the design and fabrication of the experient and the machine shop in the Physics Department at the University of Alberta for their quality work.

---

[*] Electronic address: rwolkow@ualberta.ca

[1] H. Fink, IBM journal of research and development **30**, 460 (1986).
[2] H. Fink, Physica Scripta **38**, 260 (1988).

[3] C. Chang, H. Kuo, I. Hwang, and T. Tsong, Nanotechnology **20**, 115401 (2009).

[4] B. Cho, T. Ichimura, R. Shimizu, and C. Oshima, Physical Review Letters **92**, 246103 (2004), ISSN 1079-7114.

[5] J. Pitters, R. Urban, and R. Wolkow, The Journal of Chemical Physics **136**, 154704 (2012).

[6] J. Pitters, R. Urban, S. Matsubara, and R. Wolkow (2012), submitted.

[7] R. Urban, R. Wolkow, and J. Pitters (2012), submitted.

[8] M. Silverman, L. Ballentine, et al., American Journal of Physics **76**, 1078 (2008).

[9] B. Barwick, C. Corder, J. Strohaber, N. Chandler-Smith, C. Uiterwaal, and H. Batelaan, New Journal of Physics **9**, 142 (2007).

[10] G. Stevens, M. Krüger, T. Latychevskaia, P. Lindner, A. Plückthun, and H. Fink, European Biophysics Journal pp. 1–5 (2011).

[11] G. Stevens, Journal of Microscopy **235**, 9 (2009), ISSN 1365-2818.

[12] J. Spence, W. Qian, and M. Silverman, Journal of Vacuum Science & Technology A: Vacuum, Surfaces, and Films **12**, 542 (1994), ISSN 0734-2101.

[13] M. Rezeq, J. Pitters, and R. Wolkow, The Journal of chemical physics **124**, 204716 (2006).

[14] J. Mutus, L. Livadaru, J. Robinson, R. Urban, M. Salomons, M. Cloutier, and R. Wolkow, New Journal of Physics **13**, 063011 (2011).

[15] S. P. Inc, p/N 4108PSN-BA.

[16] H. Lichte and M. Lehmann, Reports on Progress in Physics **71**, 016102 (2008).

[17] V. Georges, J. Bardon, A. Degiovanni, and R. Morin, Ultramicroscopy **90**, 33 (2001).

[18] M. Prigent and P. Morin, Journal of microscopy **199**, 197 (2000), ISSN 1365-2818.

[19] F. Hasselbach, Reports on Progress in Physics **73**, 016101 (2010).

[20] H. Lichte, Journal of electron microscopy **47**, 387 (1998).

[21] R. Fowler and L. Nordheim, Proceedings of the Royal Society of London. Series A, Containing Papers of a Mathematical and Physical Character **119**, 173 (1928).

[22] M. Scheinfein, W. Qian, and J. Spence, Journal of applied physics **73**, 2057 (1993).